

# Coordination Chemistry of Mercury(II) in Liquid and Aqueous Ammonia Solution and the Crystal Structure of Tetraamminemercury(II) Perchlorate

Kersti B. Nilsson,<sup>†</sup> Mikhail Maliarik,<sup>‡</sup> Ingmar Persson,<sup>\*,†</sup> Andreas Fischer,<sup>||</sup> Ann-Sofi Ullström,<sup>†</sup> Lars Eriksson,<sup>§</sup> and Magnus Sandström<sup>§</sup>

Department of Chemistry, Swedish University of Agricultural Sciences, P.O. Box 7015, SE-750 07 Uppsala, Sweden, IFM—Department of Chemistry, Linköping University, SE-581 83 Linköping, Sweden, Department of Chemistry, Royal Institute of Technology, SE-100 44 Stockholm, Sweden, and Department of Physical, Inorganic and Structural Chemistry, Stockholm University, SE-106 91 Stockholm, Sweden

Received July 7, 2007

The ammonia solvated mercury(II) ion has been structurally characterized in solution by means of EXAFS, <sup>199</sup>Hg NMR, and Raman spectroscopy and in solid solvates by combining results from X-ray single crystal and powder diffraction, thermogravimetry, differential scanning calorimetry, EXAFS, and Raman spectroscopy. Crystalline tetraamminemercury(II) perchlorate, [Hg(NH<sub>3</sub>)<sub>4</sub>](ClO<sub>4</sub>)<sub>2</sub>, precipitates from both liquid ammonia and aqueous ammonia solution, containing tetraamminemercury(II) complexes. The orthorhombic space group (*Pnma*) imposes C<sub>s</sub> symmetry on the tetraamminemercury(II) complexes, which is lost at a phase transition at about 220 K. The Hg–N bond distances are 2.175(14), 2.255(16), and 2 × 2.277(9) Å, with a wide N–Hg–N angle between the two shortest Hg–N bonds, 122.1(7)°, at ambient temperature. A similar distorted tetrahedral coordination geometry is maintained in liquid ammonia and aqueous ammonia solutions with the mean Hg–N bond distances 2.225(12) and 2.226(6) Å, respectively. When heated to 400 K the solid tetraamminemercury(II) perchlorate decomposes to diamminemercury(II) perchlorate, [Hg(NH<sub>3</sub>)<sub>2</sub>](ClO<sub>4</sub>)<sub>2</sub>, with the mean Hg–N bond distance 2.055(6) Å in a linear N–Hg–N unit. The mercury atoms in the latter compound form a tetrahedral network, connected by perchlorate oxygen atoms, with the closest Hg···Hg distance being 3.420(3) Å. The preferential solvation and coordination changes of the mercury(II) ion in aqueous ammonia, by varying the total NH<sub>3</sub>:Hg(II) mole ratio from 0 to 130, were followed by <sup>199</sup>Hg NMR. Solid [Hg(NH<sub>3</sub>)<sub>4</sub>](ClO<sub>4</sub>)<sub>2</sub> precipitates while [Hg(H<sub>2</sub>O)<sub>6</sub>]<sup>2+</sup> ions remain in solution at mole ratios below 3–4, while at high mole ratios, [Hg(NH<sub>3</sub>)<sub>4</sub>]<sup>2+</sup> complexes dominate in solution. The principal bands in the vibrational spectrum of the [Hg(NH<sub>3</sub>)<sub>4</sub>]<sup>2+</sup> complex have been assigned.

## Introduction

Mercury(II) complexes with monodentate ligands often display unusual and flexible coordination geometries. In the solid state, linear, trigonal, or tetrahedral arrangements of strongly bound ligand atoms are common. Octahedral coordination geometry is rather rare but occurs, e.g., with O- and N-donor ligands in solid solvates, as e.g. [Hg-

(H<sub>2</sub>O)<sub>6</sub>](ClO<sub>4</sub>)<sub>2</sub>, [Hg(OS(CH<sub>3</sub>)<sub>2</sub>)<sub>6</sub>](ClO<sub>4</sub>)<sub>2</sub>], and [Hg(NC<sub>3</sub>H<sub>5</sub>)<sub>6</sub>](CF<sub>3</sub>SO<sub>3</sub>)<sub>2</sub>, crystallizing from aqueous, dimethylsulfoxide, and pyridine solutions, respectively.<sup>1–5</sup> Anions may occasionally enter the inner coordination sphere of the mercury(II) ion as in [Hg(H<sub>2</sub>O)<sub>2</sub>(CF<sub>3</sub>SO<sub>3</sub>)<sub>2</sub>]<sub>∞</sub>, where the mercury(II) ion binds two water molecules linearly and four bridging loosely coordinated oxygen atoms from the trifluoromethanesulfonate ions to complete a tetragonally distorted octahedral

\* To whom correspondence should be addressed. E-mail: Ingmar.Persson@kemi.slu.se.

<sup>†</sup> Swedish University of Agricultural Sciences.

<sup>‡</sup> Linköping University.

<sup>||</sup> Royal Institute of Technology.

<sup>§</sup> Stockholm University.

(1) Greenwood, N. N.; Earnshaw, A. *Chemistry of the Elements*, 2nd ed.; Butterworth-Heinemann: Oxford, U.K., 1997, Chapter 29.

(2) Sandström, M.; Persson, I. *Acta Chem. Scand., Ser. A* **1978**, *32*, 95–100.

(3) Sandström, M.; Persson, I.; Åhrland, S. *Acta Chem. Scand., Ser. A* **1978**, *32*, 607–625.

coordination.<sup>6</sup> When perchlorate is used instead of trifluoromethanesulfonate as anion in pyridine solution, a neutral bis(perchlorato)tetrakis(pyridine)mercury(II) complex,  $[\text{Hg}(\text{NC}_5\text{H}_5)_4(\text{ClO}_4)_2]$ , is formed with four strong Hg–N bonds to the pyridine ligands and two markedly longer Hg–O bonds to the perchlorate oxygen atoms.<sup>7</sup> EXAFS and large angle X-ray scattering (LAXS) investigations of solvated mercury(II) ions in oxygen and nitrogen donor solvents, e.g. water, dimethyl sulfoxide, and pyridine, indicate labile six-coordination with dynamic distortions from octahedral symmetry.<sup>2–5</sup> The special coordination properties are often attributed to a contribution of the mercury(II)  $5d_{z^2}$  atomic orbital to the bonding molecular orbitals by vibronic coupling of pseudodegenerate electronic states in a pseudo Jahn–Teller (PJT) effect.<sup>8</sup>

Relativistic effects, which contract the heavy row 6 elements, have been proposed to be the cause of the special preference of mercury(II) toward linear coordination geometry, from a comparison with the different coordination behavior of cadmium(II).<sup>7</sup> A similar strong preference for linear coordination is indeed found for the isoelectronic row 6 gold(I) ion.<sup>1</sup> However, also the lighter silver(I) and copper(I) ions with a filled  $d^{10}$  shell show such a tendency. The closeness of the valence shell states, inducing vibronic coupling that destabilizes regular octahedral symmetry,<sup>8</sup> seems to be the main reason.

Mercury(II) is a typical soft electron-pair acceptor forming bonds with high degree of covalency to ligands with soft donor atoms,<sup>9,10</sup> and its special affinity to mercaptans, RSH, is well-known.<sup>1</sup> Distorted tetrahedral four-coordination is found for the mercury(II) ion in the S-donor solvent *N,N*-dimethylthioformamide with strong electron-pair donor properties,  $D_s = 52$ ,<sup>11</sup> while the solvated perchlorate salt crystallizes with a linear S–Hg–S coordination of two solvent molecules.<sup>12</sup> Also, nitrogen donor ligands can form strong bonds.<sup>7</sup> Ammonia is a solvent with very strong electron-pair donor properties as shown by the revised  $D_s$  value of 56<sup>13</sup> and is therefore expected to form strong covalent bonds to mercury(II). In aqueous ammonia, mercury(II) ions strongly favor ammonia as a ligand and form two very strong and two much weaker ammine complexes. The well-determined stability constants are  $\log K_1 = 8.8$ ,  $\log K_2 = 8.7$ ,  $\log K_3 = 1.00$ , and  $\log K_4 = 0.78$ .<sup>14,15</sup> The

second diamminemercury(II) complex,  $[\text{Hg}(\text{NH}_3)_2]^{2+}$ , dominates in a wide range of free ammonia concentration,  $\log[\text{NH}_3] = -8$  to  $-2$ , while an excess ammonia of at least ca.  $1 \text{ mol} \cdot \text{dm}^{-3}$  is required to obtain a predominating fourth complex; see Figure S1 in the Supporting Information. Recently, crystalline tetraamminemercury(II) perchlorate,  $[\text{Hg}(\text{NH}_3)_4](\text{ClO}_4)_2$ , was prepared by passing gaseous ammonia through a concentrated aqueous solution of mercury(II) perchlorate. The crystal structure at 170 K was reported with distorted tetrahedral configuration around the mercury(II) ion in the space group  $P2_1/c$ .<sup>16</sup>

The copper(I) and silver(I) ions also favor ammine ligands in aqueous ammonia and form very stable linear diammine complexes,<sup>17,18</sup> while in liquid ammonia three-coordination is achieved.<sup>18,19</sup> However, for the mercury(II) ion, the complex formation is sufficiently strong already in concentrated aqueous ammonia to sustain a dominating tetraammine complex, i.e. the same highest mercury(II) complex as in liquid ammonia.

Recent molecular dynamics simulations, based on quantum mechanically computed interactions for an inner region around the solvated ions, combined with classical molecular mechanics for the outer region (the quantum mechanics/molecular mechanics (QM/MM) method), have produced interesting insights into the structure and lability of the coordination shells and the connection between, e.g., structure breaking properties and ligand exchange rates.<sup>19</sup> Comparisons of the solvation structure and dynamics of the solvated silver(I) and gold(I) ions in aqueous and liquid ammonia solutions corroborate the preference for ammonia compared to water in mixed-ligand systems.<sup>19</sup> The common characteristics for the mercury(II), silver(I), and copper(I) ions in aqueous solutions, as shown by the QM/MM calculations, are rather labile first hydration shells with wide distributions of the coordination number and fast exchange rates. In the first shell, rapid fluctuations were found in the number of aqua ligands, which easily are replaced by other ligands. The computations for ions solvated in liquid ammonia resulted in more stable first shells, containing four ammine ligands for silver(I) and two for gold(I). The second solvation shell is large with longer residence times of the ammonia molecules than for water in the corresponding hydrated ions in aqueous solution. However, for the mercury(II) ion in ammonia solution, no such theoretical analysis has yet been reported.<sup>19</sup>

Previously, the hydrated and the dimethylsulfoxide solvated mercury(II) ions have been studied by means of <sup>199</sup>Hg NMR spectroscopy.<sup>20,21</sup> The chemical shifts reported by Peringer et al.<sup>21</sup> for solvated mercury(II) halides ( $\text{HgX}_2$ , X = Cl, Br, I) in a number of solvents covering a wide range

- (4) Persson, I.; Eriksson, L.; Lindqvist-Reis, P.; Persson, P.; Sandström, M. submitted for publication.
- (5) Åkesson, R.; Sandström, M.; Stålhandske, C. I.; Persson, I. *Acta Chem. Scand.* **1991**, *45*, 165–171.
- (6) Molla-Abbassi, A. A.; Eriksson, L.; Mink, J.; Persson, I.; Sandström, M.; Skripkin, M.; Ullström, A.-S.; Lindqvist-Reis, P. *J. Chem. Soc., Dalton Trans.* **2002**, 4357–4364.
- (7) Meyer, G.; Nockemann, P. *Z. Anorg. Allg. Chem.* **2003**, *629*, 1447–1461.
- (8) Bersuker, I. B. *Chem. Rev.* **2001**, *101*, 1067–1114.
- (9) Sandström, M.; Persson, I.; Persson, P. *Acta Chem. Scand.* **1990**, *44*, 653–675.
- (10) Marcus, Y.; Hefter, G.; Chen, T. *J. Solution Chem.* **2000**, *29*, 201–216.
- (11) Stålhandske, C. M. V.; Persson, I.; Sandström, M.; Kamienska-Piotrowicz, E. *Inorg. Chem.* **1997**, *36*, 3174–3182.
- (12) Stålhandske, C. M. V.; Stålhandske, C. I.; Sandström, M.; Persson, I. *Inorg. Chem.* **1997**, *36*, 3167–3173.
- (13) Nilsson, K. B.; Maliarik, M.; Persson, I.; Sandström, M. *Dalton Trans.*, accepted for publication.
- (14) Bjerrum, J. Thesis, University of Copenhagen, Copenhagen, 1941.

- (15) *The IUPAC Stability Constants Database*; Academic Software: Teaneck, NJ, 2000, and references therein.
- (16) Nockemann, P.; Meyer, G. *Z. Anorg. Allg. Chem.* **2003**, *629*, 123–128.
- (17) Nilsson, K. B.; Persson, I. *Dalton Trans.* **2004**, 1312–1319.
- (18) Nilsson, K. B.; Persson, I.; Kessler, V. G. *Inorg. Chem.* **2006**, *46*, 6912–6921.
- (19) Rode, B. M.; Schwenk, C. F.; Hofer, T. S.; Randolf, B. R. *Coord. Chem. Rev.* **2005**, *249*, 2993–3006.
- (20) Goodfellow, R. J. *Post-Transition Metals, Copper to Mercury*. In *Multinuclear NMR*; Mason, J., Ed.; Plenum Press: New York, 1987; Chapter 21.
- (21) Peringer, P. *Inorg. Chim. Acta* **1980**, *39*, 67–70.

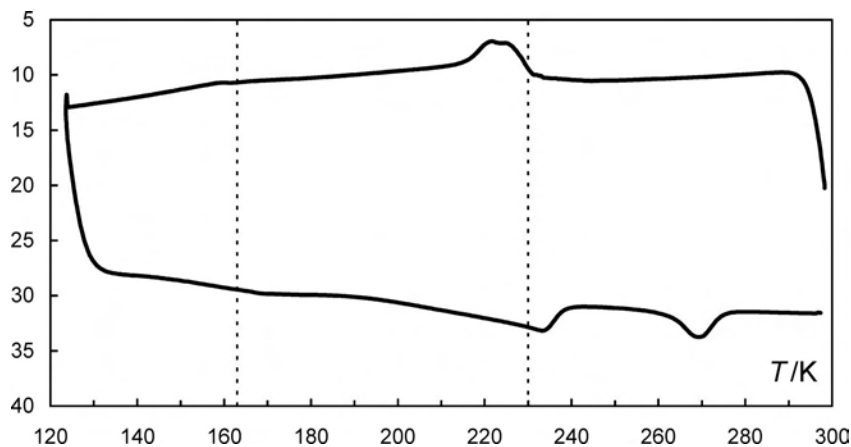


**Figure 1.** Differential scanning calorimetry of **1** in the temperature range 123.5–298.2 K. Dashed vertical bars indicate reversible phase transitions at 163 and 230 K.

of solvating ability reflect the strong solvent influence on the electron environment around the mercury atom.<sup>9,10</sup> An  $^{199}\text{Hg}$  NMR study recently performed in our laboratories also showed strong solvent dependence of the solvated mercury(II) ion in aqueous, dimethylsulfoxide, *N,N*-dimethylthioformamide, and liquid ammonia solution.<sup>22</sup> The difference in chemical shift between the tetrahedrally coordinated solvated ions in *N,N*-dimethylthioformamide and ammonia solutions and the octahedral ones in water and dimethylsulfoxide is more than 1200 ppm. An attempt was also made to correlate the spin–lattice relaxation times of the  $^{199}\text{Hg}$  nucleus in the solvated complexes with their coordination geometry.<sup>22</sup>

The current investigation characterizes the structures of the mercury(II) ammine complexes in aqueous and liquid ammonia solution, in the solid state, and also the composition and structure of the products formed when heating solid tetraamminemercury(II) perchlorate. These studies required a combination of analytical, spectroscopic, and structural techniques and were performed with the use of thermogravimetric analysis (TGA), differential scanning calorimetry (DSC), EXAFS, NMR and vibrational spectroscopy, and X-ray diffraction methods.

## Experimental Section

**Preparation of Solutions.** Liquid ammonia was prepared by distilling aqueous ammonia (25%, Merck). The ammonia vapor passed through a tube filled with dry sodium hydroxide and condensed on a “cool finger” filled with a mixture of dry ice–ethanol. To minimize uptake of water, air contact was through a tube filled with dry sodium hydroxide. The vapor pressure over pure liquid ammonia at room temperature is about 8 atm. Solutions of mercury(II) were prepared by dissolving predried anhydrous mercury(II) trifluoromethanesulfonate,  $\text{Hg}(\text{CF}_3\text{SO}_3)_2$ , prepared as described elsewhere,<sup>6</sup> or mercury(II) perchlorate trihydrate,  $\text{Hg}(\text{ClO}_4)_2 \cdot \sim 3\text{H}_2\text{O}$  (G. F. Smith), in liquid ammonia distilled either directly into 10 mm NMR tubes with PTFE valves or into glass tubes of larger size equipped with PTFE valves. The tubes were kept at a temperature of 223–233 K cooled by a dry ice–ethanol mixture in a Dewar flask. After closing the valves, the samples were kept at ambient room temperature.

The solutions of mercury(II) in aqueous ammonia were prepared in two ways. (1) Mercury(II) perchlorate trihydrate or anhydrous mercury(II) trifluoromethanesulfonate was dissolved in aqueous ammonia (25%, Merck). After some time, the solutions became opalescent, and a white and gray powder, respectively, slowly precipitated. (2) Aqueous ammonia was added to an aqueous solution of mercury(II) perchlorate immediately forming a white precipitate, which was removed from the solution by filtering and identified as  $[\text{Hg}(\text{NH}_3)_4](\text{ClO}_4)_2$  (see below). The gray precipitate from the trifluoromethanesulfonate solution, probably  $[\text{Hg}(\text{NH}_3)_4](\text{CF}_3\text{SO}_3)_2$ , was not analyzed. The mercury(II) concentration in the solutions was determined by  $^{199}\text{Hg}$  NMR spectroscopy using dimethylsulfoxide solutions of mercury(II) trifluoromethanesulfonate with known concentrations as standards for calibration of the  $^{199}\text{Hg}$  signal intensities (see below).

**Preparation of Solid Compounds.** Tetraamminemercury(II) perchlorate powder was prepared by adding aqueous ammonia under intense stirring to 0.6–0.8 mol·dm<sup>-3</sup> aqueous solutions of mercury(II) perchlorate, to a mole ratio of  $\text{NH}_3:\text{Hg} \approx 4$ . The white precipitate formed was filtered off, washed with water, and dried in a vacuum desiccator over silica gel until constant weight.

Crystalline tetraamminemercury(II) perchlorate,  $[\text{Hg}(\text{NH}_3)_4](\text{ClO}_4)_2$  (**1**), was prepared in two ways: (1) A solution of mercury(II) perchlorate in liquid ammonia was cooled to ca. 225 K and transferred into an 1 mL screw-thread glass vial with a PTFE/silicone septum, thickness 2 mm. When slowly raising the temperature, the ammonia evaporated through a micro hole made in the septum leaving crystals of the title compound. (2) A saturated solution of mercury(II) perchlorate in aqueous ammonia, 0.11 mol·dm<sup>-3</sup>, was prepared at room temperature and cooled to ca. 278 K. After a few hours, crystals of **1** started to form. The compound **1** is stable in ammonia atmosphere but decomposes slowly in air, making elemental analysis difficult. A thermogravimetric study provided more useful information; see below.

Diamminemercury(II) perchlorate powder,  $\{[\text{Hg}(\text{NH}_3)_2](\text{ClO}_4)_2\}_n$  (**2**), is a stable deammoniated compound that forms after extended storage in air or gentle heating of tetraamminemercury(II) perchlorate; see the results below from vibrational spectroscopy. X-ray powder diffraction (XRD) showed that **2** was the product formed during the thermogravimetric analysis made on **1**, after heating to 543 K and then cooling to 153 K for 18 h.

Tetraamminemercury(II) trifluoromethanesulfonate,  $[\text{Hg}(\text{NH}_3)_4](\text{C}_3\text{FSO}_3)_2$  (**3**), formed as colorless crystals from a liquid ammonia solution of mercury(II) trifluoromethanesulfonate in the same way as

(22) Maliarik, M.; Persson, I. *Magn. Reson. Chem.* **2005**, *43*, 835–842.

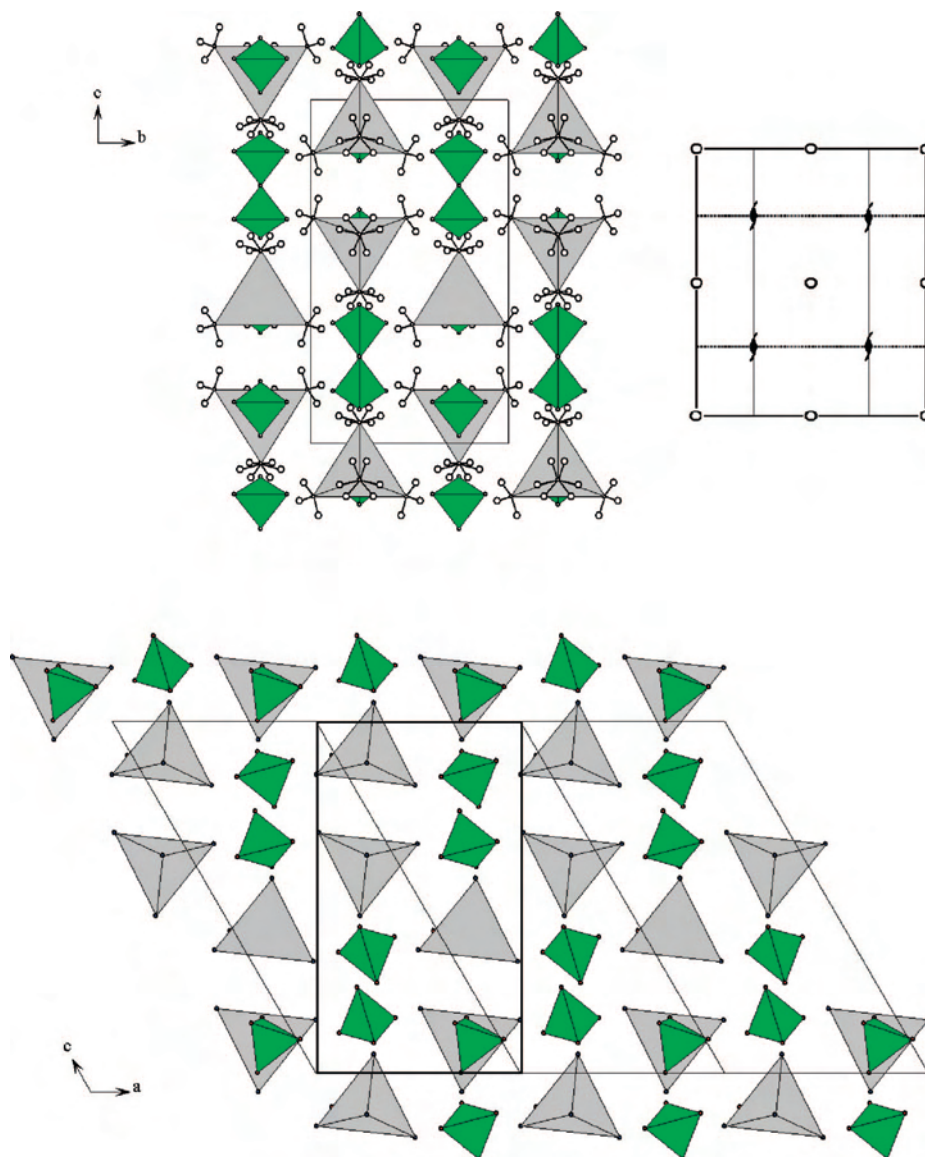


**Figure 2.**  $[\text{Hg}(\text{NH}_3)_4](\text{ClO}_4)_2$  crystal structures. (upper) Projection along the  $a$  axis of the room temperature orthorhombic unit cell ( $Pnma$ , present work) with a description of symmetry elements (mirror planes and screw axes), as found in International Tables for Crystallography (part C). (lower) Projection along the  $b$  axis of the monoclinic low temperature phase ( $P2_1/c$ , ref 16). Note the absence of a mirror plane perpendicular to the  $a$  axis and that the remaining 2-fold screw axes have been shifted  $1/4$  in the  $a$  direction. Green and gray tetrahedra represent  $\text{ClO}_4^-$  and  $\text{Hg}(\text{NH}_3)_4^{2+}$ , respectively.

described for **1** above. A saturated solution of mercury(II) trifluoromethanesulfonate in aqueous ammonia yielded the same compound. The crystals are very unstable, both in air and in paraffin oil, and no attempt to perform a crystallographic structure determination was made.

**Caution!** Although no problems were experienced with the present samples, perchlorates in nonaqueous solvents are potentially explosive.

**Single Crystal X-ray Diffraction.** Single crystals of **1**, grown by the two preparative routes described above, were selected and mounted into glass capillaries with paraffin oil. The crystals were spherically shaped, 0.20–0.30 mm in diameter. Data collections were performed at  $295 \pm 1$  K by means of a Oxford diffraction Excalibur-II Kappa diffractometer equipped with a Sapphire-III CCD and a Bruker SMART CCD diffractometer.<sup>23,24</sup> Numerical absorption corrections were applied.<sup>25</sup> The

structure was solved by direct methods and refined by means of the full-matrix least-squares method on  $F^2$  in SHELXL-97.<sup>26</sup> All non-hydrogen atoms were refined anisotropically. The three hydrogen atoms of the ammine groups were geometrically positioned and refined using a riding model that allowed twisting motions.

**X-ray Powder Diffraction.** The white powder of **2** was measured in transmission mode geometry on a STOE powder diffractometer equipped with a Ge monochromator set to diffract  $\text{Cu K}\alpha_1$  radiation ( $\lambda \approx 1.54060 \text{ \AA}$ ).<sup>27</sup> The extracted peak positions were indexed on a cubic  $F$ -centered unit cell with TREOR,<sup>28</sup> and

(23) Xcalibur CCD system, CrysAlis Software system, version 1.17; Oxford Diffraction Ltd.: Blacksburg, VA, 2003.

(24) Bruker SMART and SAINT, area detector control and integration software, Bruker Analytical X-ray Systems: Madison, WI, 1995.

(25) Herrendorf, W.; Bärnighausen, H. *HABITUS, a program for numerical absorption correction*; Universities of Giessen and Karlsruhe: Germany, 1997.

(26) Sheldrick, G. M. *Acta Crystallogr., Sect. A* **1990**, *46*, 467–473.

(27) STOE & Cie GmbH, Hilpertstr. 10, D-64295 Darmstadt, Germany.

(28) Werner, P.-E.; Eriksson, L.; Westerdahl, M. *J. Appl. Crystallogr.* **1985**, *18*, 367–370.

**Table 1.** Selected Crystallographic Data for the Tetraamminemercury(II) and Diamminemercury(II) Perchlorate Compounds<sup>a</sup>

compound	$[\text{Hg}(\text{NH}_3)_4](\text{ClO}_4)_2$	$[\text{Hg}(\text{NH}_3)_2](\text{ClO}_4)_2$
empirical formula	$\text{H}_{12}\text{Cl}_2\text{N}_4\text{O}_8\text{Hg}$	$\text{H}_6\text{Cl}_2\text{N}_2\text{O}_8\text{Hg}$
formula weight	467.61	433.57
crystal size/mm	$0.30 \times 0.25 \times 0.20$	powder
wavelength/Å	0.71073	1.5406
crystal system	orthorhombic	cubic
space group	<i>Pnma</i> (no. 62)	<i>Fd<math>\bar{3}m</math></i> (no. 227)
<i>a</i> /Å	10.8918(14)	9.7596(7)
<i>b</i> /Å	8.031(3)	
<i>c</i> /Å	13.847(3)	
volume/Å <sup>3</sup>	1211.2(5)	929.6(1)
<i>Z</i>	4	3.76 (occupancy of Hg refined)
<i>D<sub>c</sub></i> /g·cm <sup>-3</sup>	2.564	
temperature/K	293	293
<i>m</i> (Mo Kα)/mm <sup>-1</sup>	13.177	
absorption correction	empirical method	
transmission factors	0.384, 0.5913	
<i>F</i> (000)	872	436.6
<i>q</i> <sub>max</sub> /deg	31.95	64.98
<i>h, k, l</i>	±10, ±7, -13 - +7	
independent reflections	2083	
reflections with <i>I</i> > 2σ( <i>I</i> )	1053	
<i>N</i> <sub>par</sub> , <i>N</i> <sub>stepint</sub>		24, 3125
<i>R</i> <sub>int</sub> /percent	6.4	
completeness to θ 25.00°/percent	99.5	
refinement method	full-matrix least-squares on <i>F</i> <sup>2</sup>	Rietveld refinement
data/restraints/parameter	2083/30/76	
goodness-of-fit on <i>F</i> <sup>2</sup>	1.069	
final <i>R</i> indices ( <i>I</i> > 2σ)	<i>R</i> <sub>1</sub> = 0.0578 <i>wR</i> <sub>2</sub> = 0.1743	
<i>R</i> indices (all data)	<i>R</i> <sub>1</sub> = 0.1110 <i>wR</i> <sub>2</sub> = 0.2227	
<i>R</i> - <i>p</i> , <i>R</i> - <i>wp</i> , <i>R</i> - <i>F</i> , DW		0.17, 0.26, 0.0784, 0.86
largest diff. peak and hole/e·Å <sup>-3</sup>	2.01 to -1.43	1.81 to -0.53

<sup>a</sup> Definition of *R*: SHELX  $R_1 = \sum |F_o| - |F_c| / \sum |F_o|$ ;  $wR_2 = (\sum [w(F_o^2 - F_c^2)^2] / \sum [w(F_o^2)^2])^{1/2}$ .

the structure was solved using the program EXPO.<sup>29</sup> Several initial models in different space groups were tested by means of Fullprof.<sup>30</sup> The final model was obtained from Rietveld refinement using Fullprof. The electron density maps were calculated with both EXPO and SHELXL97, and several different residual peaks were tested but rejected as possible atoms. From the Rietveld refinements, the structure factor residual,  $R(F) = 0.0784$  was derived with only two atoms in the final model: one mercury and one chlorine atom. No other atoms could be located due to severe disorder. The estimated standard deviations should be multiplied by a factor of 3.56 due to serial correlations.<sup>31</sup> The density of the powder was measured with a Micromeritics Accupyc 1330 Helium Pycnometer (Micromeritics Corporate Headquarters, Norcross, GA).

**EXAFS Data Collection.** Mercury L<sub>III</sub>-edge X-ray absorption spectra were recorded at the wiggler beam line 4-1 at the Stanford Synchrotron Radiation Laboratory (SSRL) on two occasions. The storage ring was operated at 3.0 GeV with a maximum current of 100 mA. The data collection was performed in transmission mode at ambient temperature by means of an energy scan with a Si[220] double crystal monochromator. Higher order harmonics in the X-ray beam were reduced by detuning the second monochromator to 50% of maximum intensity at the end of the scans. The liquid ammonia solution of mercury(II) perchlorate was cooled to ca. 200 K with the use of a liquid nitrogen-ethanol mixture as described else-

where,<sup>18</sup> and during the EXAFS scans, a slow temperature increase took place. The solid samples were kept in 1–1.5 mm thick silver frames with Mylar tape windows and were diluted with boron nitride to give an edge step of about one unit in the logarithmic intensity ratio. The aqueous ammonia solution was contained between 6 μm polypropylene X-ray film windows in a cell with a 5 mm Vitone spacer. The energy scale of the X-ray absorption spectra was calibrated by assigning the first inflection point of the L<sub>3</sub> edge of solid mercury(II) chloride, diluted with BN, to 12284 eV.<sup>32</sup> For each sample at least 3 scans were averaged, giving satisfactory data (*k*<sup>3</sup>-weighted) up to *k* ≈ 10 Å<sup>-1</sup> (*k* ≈ 15 Å<sup>-1</sup> for the  $[\text{Hg}(\text{NH}_3)_2](\text{ClO}_4)_2$  compound). The EXAFSPAK program package was used for all data treatment and refinement of structural parameters.<sup>33</sup>

**EXAFS Data Analysis.** The EXAFS oscillations were extracted from the spectra after performing standard procedures for pre-edge subtraction and spline removal. Model functions were obtained using ab initio calculated phase and amplitude parameters by FEFF7 (version 7.02).<sup>34</sup> Input to the FEFF7 program was prepared from

- (29) Altomare, A.; Caliendo, R.; Camalli, M.; Cuocci, C.; Giacobozzo, C.; Moliterni, A. G. G.; Rizzi, R. *J. Appl. Crystallogr.* **2004**, *37*, 1025–1028.  
 (30) Rodriguez-Carvajal, J. FULLPROF: A Program for Rietveld Refinement and Pattern Matching Analysis. *Abstracts of the Satellite Meeting on Powder Diffraction of the XV Congress of the IUCr*, Toulouse, France, **1990**; p 127.  
 (31) (a) Berar, J. F.; Lelann, P. *J. Appl. Crystallogr.* **1991**, *24*, 1–5. (b) Berar, J. F. *Powder Diffraction II* **1992**, *846*, 63.

- (32) Thompson, A.; Attwood, D.; Gullikson, E.; Howells, M.; Kim, K.-J.; Kirz, J.; Kortright, J.; Lindau, I.; Pianatta, P.; Robinson, A.; Scofield, J.; Underwood, J.; Vaughan, D.; Williams, G.; Winick, H. *X-ray Data Booklet*; LBNL/PUB-490, Lawrence Berkeley National Laboratory: Berkeley, CA, 2001; Rev. 2.  
 (33) George, G. N.; Pickering I. J. *EXAFSPAK - A Suite of Computer Programs for Analysis of X-ray Absorption Spectra*; Stanford Synchrotron Radiation Laboratory: Stanford, CA, 1993.  
 (34) (a) FEFF code for ab initio calculations of XAFS: Zabinsky, S. I.; Rehr, J. J.; Ankudinov, A.; Albers, R. C.; Eller, M. J. *Phys. Rev. B* **1995**, *52*, 2995–3009. (b) Ankudinov, A. Ph.D. Thesis, University of Washington, 1996. (c) The FEFF program is available from <http://feff.phys.washington.edu/feff>.

**Table 2.** Results of Curve-Fitting to  $k^3$ -Weighted Hg L<sub>3</sub>-Edge EXAFS Data<sup>a</sup>

sample	scattering path	<i>N</i>	<i>d</i>	$\sigma^2$	<i>E</i> <sub>0</sub>	<i>S</i> <sub>0</sub> <sup>2</sup>
[Hg(NH <sub>3</sub> ) <sub>4</sub> ] <sup>+</sup> in NH <sub>3</sub> (aq)	Hg–N	4	2.226(2)	0.0088(2)	12289.3(3)	0.83(2)
	Hg–N–N	12	3.89(2)	0.014(4)		
[Hg(NH <sub>3</sub> ) <sub>4</sub> ] <sup>+</sup> in NH <sub>3</sub> (l)	Hg–N	4	2.225(4)	0.0023(5)	12289.3(7)	0.67(4)
	Hg–N–N	12	4.02(2)	0.0087(13)		
<b>1</b> [Hg(NH <sub>3</sub> ) <sub>4</sub> ](ClO <sub>4</sub> ) <sub>2</sub> (s)	Hg–N	4	2.229(2)	0.0075(8)	12289.6(3)	0.70(2)
	Hg–N–N	12	3.96(2)	0.01(2)		
<b>2</b> [Hg(NH <sub>3</sub> ) <sub>2</sub> ](ClO <sub>4</sub> ) <sub>2</sub> (s)	Hg–N	2	2.055(2)	0.0012(2)	12289.2(4)	0.70(3)
	Hg•••Hg	6	3.420(1)	0.0038(1)		
	Hg•••Hg	12	5.955(8)	0.0111(7)		
	Hg•••Cl	4	4.063(12)	0.014(2)		
	Hg–O	4	2.840(9)	0.0107(12)		

<sup>a</sup> The model parameters are frequency (*N*), mean bond distances (*d*/Å), disorder (Debye–Waller) parameter ( $\sigma^2/\text{Å}^2$ ), threshold energy (*E*<sub>0</sub>/eV), and amplitude reduction factor (*S*<sub>0</sub><sup>2</sup>).

the crystal structure of **1** for the four-coordinated compounds and by assuming appropriate angles and distances for **2**, supported by the X-ray powder diffraction analysis.

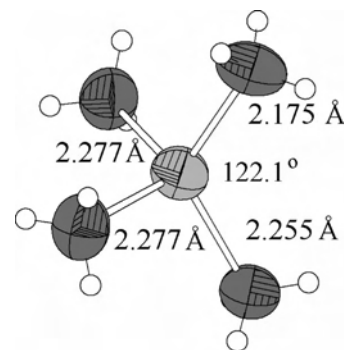
The standard deviations given for the refined parameters in Table 2 of the model functions are obtained from a least-squares fit to the  $k^3$  weighted EXAFS oscillations  $\chi(k)$  and do not include systematic errors of the measurements. However, the estimated statistical errors allow comparisons, e.g., of the relative shifts in the distances. The variations in the refined parameters, using different models and data ranges including the shift in the *E*<sub>0</sub> value (for which  $k = 0$ ), indicate that the accuracy of the distances obtained for well-defined atom-pair interactions in the complexes is within  $\pm 0.01$ – $0.02$  Å. The estimated errors given in the text have been increased accordingly to include effects of systematic deviations.

**NMR Measurements.** <sup>199</sup>Hg NMR spectra were recorded at 71.33 MHz (9.4 T) on Bruker AM400 and DRX400 spectrometers. The <sup>199</sup>Hg chemical shifts in the spectra were referred to the resonance of 0.1 mol·dm<sup>−3</sup> mercury(II) perchlorate in 0.1 mol·dm<sup>−3</sup> perchloric acid at 293 K.<sup>20</sup> The samples containing liquid ammonia were kept in either 5 or 10 mm NMR tubes, closed with PTFE valves. The temperature dependence of the chemical shift was determined in the range 203–303 K for a liquid ammonia solution of mercury(II) trifluoromethanesulfonate and from 293 to 323 K for an acidified aqueous solution of mercury(II) perchlorate, respectively. The spin–lattice relaxation times at 298 K of <sup>199</sup>Hg in the solvates were determined by the inversion–recovery technique with the standard Bruker *T*<sub>1</sub> program within the XWinNMR 3.0 software package. In all experiments, the actual 90° pulse was determined. The line widths of the signals were determined by fitting single Lorentzians to each observed signal, and integrals of the signal intensities were obtained using the XWinNMR 3.0 program. The data were evaluated by means of the nonlinear curve fitting option of the ORIGIN 4.0 program (Microcal Software, Inc.) for the three parameter exponential equation:<sup>35</sup>

$$I_{\tau} = A + B \exp(-\tau/T_1)$$

For quantitative measurements of the <sup>199</sup>Hg signal intensities, 30–60° flip angles were used with a time delay between the pulses of  $(1-2) \times T_1$  at the current magnetic field (see below).

**Vibrational Spectroscopy.** Raman spectra of the solid samples were measured using a Renishaw System 1000 spectrometer, equipped with a Leica DMLM microscope, a 25 mW diode laser (782 nm), and a Peltier-cooled CCD detector. Raman spectra of the powders were recorded by means of the FT-Raman accessory of a Bio-RAD FTS 6000 FT-IR spectrometer and the FT-Raman

**Figure 3.** Tetraamminemercury(II) ion in the crystal structure of **1**.

module FRA106/S combined with the Bruker IFS66/S FT-IR spectrometer. The 1024 nm line from Nd:YAG-lasers was used to irradiate the samples with 700–1200 mW, collecting 10–200 scans at a spectral bandwidth of 2–4 cm<sup>−1</sup>. The infrared absorption spectra of the samples as Nujol mulls were measured by means of a Perkin-Elmer 1720 FT-IR spectrometer, using KBr windows.

**Thermogravimetry.** The TGA studies were performed on a Perkin-Elmer TGA7 instrument. About 6–9 mg of sample was heated in an Ar atmosphere in an open platinum crucible at a rate of 5 K·min<sup>−1</sup> in the temperature range 293–543 K and at 10 K·min<sup>−1</sup> in the range 543–873 K.

**Differential Scanning Calorimetry (DSC).** The DSC measurement was performed with a Perkin-Elmer DSC Pyris 1 instrument. Phase transitions were investigated by monitoring the energy absorbed or released when cooling ca. 10 mg of **1** from 298 to 123 K at a rate of 5 K·min<sup>−1</sup>, followed by a temperature increase to 298 K.

## Results and Discussion

**Structure and Properties of Solid [Hg(NH<sub>3</sub>)<sub>4</sub>](ClO<sub>4</sub>)<sub>2</sub>.** Differential scanning calorimetry (DSC) reveals a composite exothermic phase transition when cooling crystals of compound **1** below ca. 220 K, Figure 1. When heating, the phase transition separates into two steps, at about 230 K and at ca. 270 K. The crystal structure of **1** at 295 K (orthorhombic space group *Pnma*) shows a similar molecular arrangement as that reported at 170 K for a monoclinic unit cell (space group *P2<sub>1</sub>/c*), with tetraamminemercury(II) complexes hydrogen bonded to surrounding perchlorate ions (Figure 2).<sup>16</sup> The projections along the *a* and *b* axes of the high and low temperature phases, respectively, show essentially the same positions of the Hg and Cl atoms. However, the mirror planes of the orthorhombic space group *Pnma* impose *C*<sub>s</sub> symmetry on both the tetraamminemercury(II) complexes and perchlo-

(35) Braun, S.; Kalinowski, H.-O.; Berger, S. In *100 and More Basic NMR Experiments*; Vch Publishers: New York, 1996.

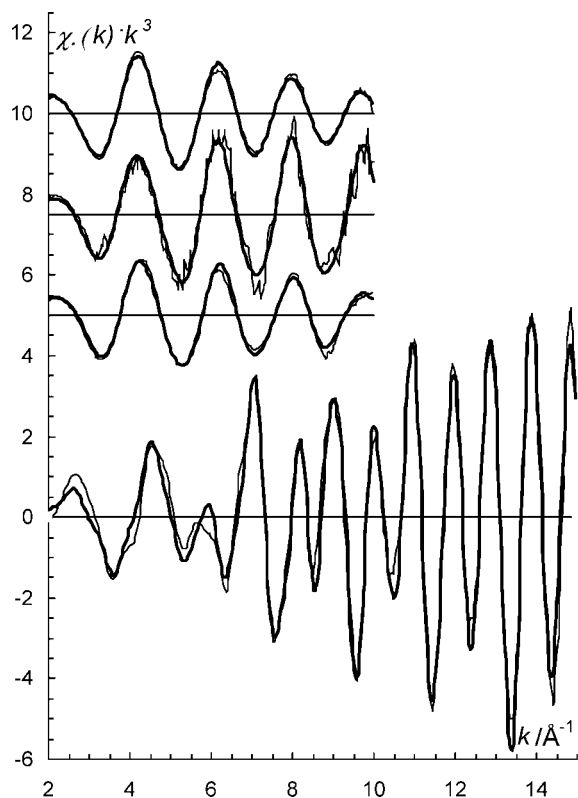


**Figure 4.** EXAFS data ( $k^3$ -weighted) and experimental (solid thin line) and fitted model function (solid thick line) for the following:  $[\text{Hg}(\text{NH}_3)_4]^{2+}$  in  $\text{NH}_3(\text{aq})$ , (offset 10);  $[\text{Hg}(\text{NH}_3)_4]^{2+}$  in  $\text{NH}_3(\text{l})$ , (offset 7.5);  $[\text{Hg}(\text{NH}_3)_4](\text{ClO}_4)_2$ , (offset 5); and  $[\text{Hg}(\text{NH}_3)_2](\text{ClO}_4)_2$  (no offset).

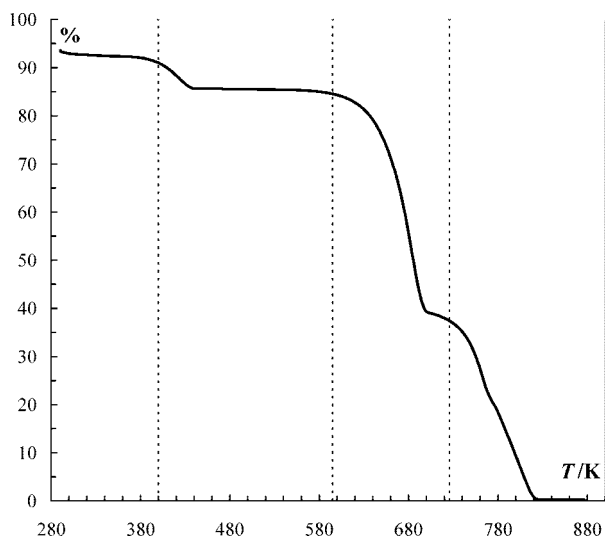


**Figure 5.** Thermogravimetric analysis of **1**. The dashed vertical bars indicate the decomposition temperatures 400 K for **1** and 595 K for **2**.

rate ions, which are absent in the monoclinic space group  $P2_1/c$ . The main difference is found in the orientation of the corresponding polyhedra. The tetraamminemercury(II) complex of **1** shows the Hg–N bond distances, 2.175(14), 2.255(16), and  $2 \times 2.277(9)$  Å, with a rather wide N–Hg–N angle between the two shortest Hg–N bonds,  $122.1(7)^\circ$ , Figure 3. The perchlorate ions are also located on the  $a$ – $c$  mirror planes with the oxygen atoms hydrogen bonded to the ammine groups, Table S1 in the Supporting Information. At 170 K, after the phase transition to the low temperature

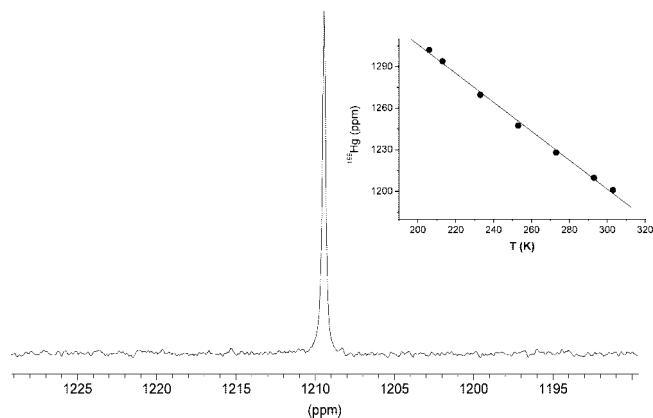


**Figure 6.**  $^{199}\text{Hg}$  NMR spectrum of an  $0.3 \text{ mol} \cdot \text{dm}^{-3}$  liquid ammonia solution of  $\text{Hg}(\text{CF}_3\text{SO}_3)_2$ . (inset) Temperature dependence of the  $^{199}\text{Hg}$  NMR chemical shifts of the ammonia solvated mercury(II) ion.

monoclinic space group for which no hydrogen positions were reported,<sup>16</sup> the alignment of the polyhedra disappears (Figure 2). The Hg–N bond distances show small changes and are reported as 2.241(15), 2.247(14), 2.287(15), and 2.287(15) Å without mirror symmetry and with the N–Hg–N bond angle  $125.0(6)^\circ$  between the two shortest Hg–N bonds.<sup>16</sup> However, it is possible that the mirror symmetry in the high temperature orthorhombic cell may actually result from an average of two alternative orientations, each similar to the one at low temperature. Such a model would be consistent with the two alternative orientations found for the hydrogen atoms of the ammine group on the mirror plane (Figure 2).

Thus, the phase transitions with different activation energies revealed by the DSC experiment could correspond to flipping motions of the polyhedra. It seems probable that a reorientation takes place collectively in domains rather than by individual dynamic motions, possibly with a corresponding reorientation of the hydrogen bonds in a second step. Selected crystallographic and experimental details are given in Table 1, and the crystallographic data in CIF format are available in the Supporting Information.

The Hg–N bond distances are too close to be separated in an EXAFS data analysis, and only a mean distance can be obtained. The model fitting to the EXAFS data of **1** gives a mean value  $2.229(6)$  Å (Table 2), which is not significantly different from the average Hg–N bond distance from the crystal structure, 2.246 Å, at ambient temperature. The average value from the low temperature crystal structure is somewhat longer, 2.266 Å, which could be an indication of better defined molecular orientations and atomic positions. However, it is surprising that the EXAFS value, which is independent of disorder effects, is so much lower. The disorder (Debye–Waller) parameter of the mean EXAFS Hg–N bond distance,  $\sigma^2 = 0.0075(9)$  Å<sup>2</sup> (Table 2), is larger than usual for regular tetrahedral configuration but is consistent with the distribution of Hg–N bond distances obtained in the crystallographic study. The fit of the model to the EXAFS data of **1** is visualized in Figure 4 and the XANES spectrum is in Figure S2 in the Supporting Information.

**Table 3.**  $^{199}\text{Hg}$  NMR Parameters at 9.40 T and 298 K for 0.3 mol·dm $^{-3}$  Solutions of Solvated Mercury(II) Species

solvate (solution)	solvent	$C_{\text{Hg}^{2+}}$ (mol·dm $^{-3}$ )	$\delta$ (ppm)	$T_1$ (s)	temp coeff (ppm·K $^{-1}$ )	ref
[Hg(H $_2$ O) $_6$ ] $^{2+a}$	0.1 mol·dm $^{-3}$ HClO $_4$ (aq)	0.3	−1.4	7.63 ± 0.47	−0.40	22
[Hg(OS(CH $_3$ ) $_2$ ) $_6$ ] $^{2+}$	dimethylsulfoxide	0.3	−65.8	6.62 ± 0.45	−0.31	22
[Hg(SCHN(CH $_3$ ) $_2$ ) $_4$ ] $^{2+}$	<i>N,N</i> -dimethylthioformamide	0.3	1664	2.61 ± 0.08	−0.75	22
[Hg(NH $_3$ ) $_4$ ] $^{2+b}$	liquid ammonia	0.3	1209	3.00 ± 0.09	−1.04	22 $^f$
[Hg(NH $_3$ ) $_4$ ] $^{2+a}$	liquid ammonia	0.4	1207			<i>f</i>
[Hg(NH $_3$ ) $_4$ ] $^{2+a,c}$	aqueous ammonia	0.11	1204			<i>f</i>
[Hg(NH $_3$ ) $_4$ ] $^{2+a,d}$	aqueous ammonia	0.09	1205			<i>f</i>
[Hg(NH $_3$ ) $_4$ ] $^{2+a,e,f}$	aqueous ammonia	0.05	1179	3.23 ± 0.31		<i>f</i>

$^a$  Solute: Hg(ClO $_4$ ) $_2$ · $\sim$ 3H $_2$ O.  $^b$  Solute: Hg(CF $_3$ SO $_3$ ) $_2$ .  $^c$  NH $_3$ /Hg(II)  $\approx$  110.  $^d$  NH $_3$ /Hg(II)  $\approx$  130.  $^e$  NH $_3$ /Hg(II)  $\approx$  50.  $^f$  This work.

A thermogravimetric analysis (TGA) was performed of crystals of **1** stored in ammonia atmosphere. When the excess of adsorbed ammonia evaporated a plateau corresponding to the tetraamminemercury(II) perchlorate **1** was reached at 340 K at a heating rate of 5 K·min $^{-1}$ . At this temperature, 92.1% of the starting mass remained and the weight of the sample kept constant up to 380 K, Figure 5. With increasing temperature, **1** gradually loses two additional ammonia molecules. The diamminemercury(II) perchlorate **2**, 85.5% (exp) 85.5% (calc), has a stability range of almost 200 K, starting at 444 K, before it decomposes further. In another experiment, **1** was kept at 333 K for 30 min, before recording its EXAFS spectrum. The Fourier transform (Figure S3 in the Supporting Information) shows incomplete deammoniation of **1** to **2**, consistent with the thermogravimetric study.

**Tetraamminemercury(II) Complex in Aqueous and Liquid Ammonia Solution.** The raw Hg L $_{\text{III}}$  EXAFS spectra of **1** and the aqueous ammonia solution of mercury(II) perchlorate are similar, while the liquid ammonia solution displays the same phase but much larger amplitude of the oscillations, Figure 4. The structure of the Hg L $_{\text{III}}$  absorption edges of **1** and of the liquid and aqueous ammonia solutions of mercury(II) perchlorate are almost identical; see Figure S2 in the Supporting Information. Thus, the same mercury(II) species, i.e. the [Hg(NH $_3$ ) $_4$ ] $^{2+}$  complex, must be dominating in concentrated aqueous ammonia solution and also in liquid ammonia as the low temperature results in lower Debye–Waller coefficients and thereby larger amplitudes. The mean Hg–N bond distance was obtained as 2.225(12) and 2.226(6) Å in liquid and aqueous ammonia solution, respectively, with the corresponding disorder parameters  $\sigma^2 = 0.0023(5)$  and 0.0088(2) Å $^2$ , Table 2. To conclude, the structure of the [Hg(NH $_3$ ) $_4$ ] $^{2+}$  complex in **1** is maintained in aqueous ammonia solution, with similar large disorder parameters that implicate rather wide distributions of the Hg–N distances. In the liquid ammonia solution, the dominating scattering pathway is also Hg–N, with a similar mean bond distance. The small disorder parameter shows much smaller vibrational amplitude and also smaller distribution of the Hg–N distances at the lower temperature.

Liquid ammonia solutions of mercury(II) trifluoromethanesulfonate, 0.2–0.7 mol·dm $^{-3}$ , were studied by  $^{199}\text{Hg}$  NMR spectroscopy, and at 298 K, a single  $^{199}\text{Hg}$  NMR resonance was obtained at 1209 ppm without noticeable concentration dependence (Figure 6). The temperature dependence of the signal is significant, however, and in the range 203–303 K, the chemical shift decreases linearly with increasing tem-

perature with a temperature coefficient of −1.04 ppm·K $^{-1}$  (Figure 6, inset), while there is little change in the line width, from 4 to 9 Hz. The lack of spin–spin coupling,  $J(^{199}\text{Hg}–^{1}\text{H})$  or  $J(^{199}\text{Hg}–^{14}\text{N})$ , in the spectra is attributed to fast exchange of ammonia molecules between the first coordination shell of the mercury(II) ion and bulk solvent $^{19,36}$  and also to the fast relaxation due to scalar coupling to the quadrupolar  $^{14}\text{N}$  nuclei in the ammonia molecule. $^{37}$  Thus, no direct information can be deduced on the composition and the structure of the solvate. However, all observations are consistent with a single predominating mercury species in the solutions and the EXAFS results allow the observed signal to be attributed to the tetraamminemercury(II) ion.

Also for the 0.4 mol·dm $^{-3}$  solution of mercury(II) perchlorate trihydrate in liquid ammonia, a single  $^{199}\text{Hg}$  resonance with the same chemical shift (1207 ppm) was observed (cf. Table 3), indicating that neither the presence of some water in large ammonia excess nor the perchlorate anions influence the formation of the tetraamminemercury(II) complex. However, in aqueous ammonia, the chemical shift decreases somewhat for decreasing NH $_3$ /Hg(II) mole ratios ( $\leq 100$ ; see Table 3).

The  $^{199}\text{Hg}$  chemical shift strongly depends on the geometry and coordination number of the mercury(II) ion in its solvated complexes. $^{22}$  For the octahedrally solvated mercury(II) ions in aqueous and dimethyl sulfoxide solution, [Hg(OH $_2$ ) $_6$ ] $^{2+}$  and [Hg(OS(CH $_3$ ) $_2$ ) $_6$ ] $^{2+}$ , the  $\delta$  ( $^{199}\text{Hg}$ ) values are 0 (reference) and −66 ppm, respectively, and 1664 ppm for the four-coordinated pseudotetrahedral solvated mercury(II) ion in *N,N*-dimethylthioformamide, [Hg(SCHN(CH $_3$ ) $_2$ ) $_4$ ] $^{2+}$ , (Table 3). Ligands with sulfur donor atoms generally deshield the mercury(II) nucleus more efficiently than nitrogen and oxygen atoms. $^{38,39}$  Therefore, the smaller increase in the relative  $^{199}\text{Hg}$  chemical shift (1207 ppm) of the solvated mercury(II) ion in liquid ammonia supports a tetrahedral configuration of the tetraamminemercury(II) complex, [Hg(NH $_3$ ) $_4$ ] $^{2+}$ .

The  $^{199}\text{Hg}$  spin–lattice relaxation times for the hydrated, and the dimethylsulfoxide, *N,N*-dimethylthioformamide and ammonia solvated mercury(II) ions, were measured at the same concentration, temperature, and magnetic field. The

(36) Helm, L.; Merbach, A. E. *Coord. Chem. Rev.* **1999**, *187*, 151–181.

(37) Aikitt, J. W.; Mann, B. E. *NMR and Chemistry*, 4th ed.; Stanley Thomes, Cheltenham, 2000.

(38) Utschig, L. M.; Bryson, J. W.; O'Halloran, T. V. *Science* **1995**, *268*, 380–385.

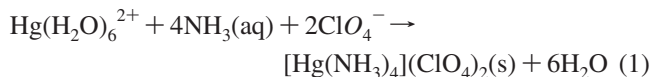
(39) Huffman, D. L.; Utschig, L. M.; O'Halloran, T. V. *Metal Ions Biol. Syst.* **1997**, *34*, 503–526.



slightly distorted  $[\text{Hg}(\text{NH}_3)_4]^{2+}$  and  $[\text{Hg}(\text{SCHN}(\text{CH}_3)_2)_4]^{2+}$  species obtained similar  $T_1$  values, 3.00 and 2.61 s, respectively, while the relaxation times of the pseudo-octahedral species,  $[\text{Hg}(\text{OH}_2)_6]^{2+}$  and  $[\text{Hg}(\text{OS}(\text{CH}_3)_2)_6]^{2+}$ , are substantially longer, 7.6 and 6.6 s, respectively, Table 3.

#### Mercury(II) Perchlorate–Aqueous Ammonia System.

The filtrates obtained when removing the white precipitate of **1** formed after adding different amounts of aqueous ammonia to aqueous solutions of mercury(II) perchlorate (see above) have been studied by  $^{199}\text{Hg}$  NMR. The mercury speciation in the solution depends on the original net mole ratio  $R = n(\text{NH}_3)/n(\text{Hg}^{2+})$  in the heterogeneous system. For  $R = 2$ , a single  $^{199}\text{Hg}$  NMR resonance at  $-3$  ppm indicates that the hydrated mercury(II) ion,  $[\text{Hg}(\text{H}_2\text{O})_6]^{2+}$ , is the only detectable mercury(II) species remaining in solution and that almost all ammonia has been removed as the precipitate **1** (cf. Table 3). The lack of noticeable hydrolysis is due to the high acidity ( $\text{pH} = 1.5$ ) persisting in the aqueous phase for  $R \leq 2$ . When increasing the amount of ammonia up to  $R \sim 4$ , tetraamminemercury(II) perchlorate precipitates almost quantitatively and no mercury(II) species in solution could be detected by  $^{199}\text{Hg}$  NMR. Thus, the main reaction is the following:



The corresponding changes in the UV–vis spectra when adding aqueous ammonia to the solutions are shown in Figure S4 in the Supporting Information. A broad band centered at  $\sim 240$  nm, also appearing in the original aqueous solution of mercury(II) perchlorate, should be attributed to the hydrated mercury(II) ion (cf. Figure S4a and b). In the systems with  $R \geq 4$ , no  $[\text{Hg}(\text{H}_2\text{O})_6]^{2+}$  species could be detected in the solution by means of  $^{199}\text{Hg}$  NMR and the 240 nm band in UV is absent (Figure S4c). UV–vis spectroscopy was not able to distinguish further between the species. For  $R > 6$ , a strong absorption band at  $\lambda < \sim 220$  nm from ammonia rapidly grows and prevents the detection of bands from the mercury(II) complexes (cf. Figure S4d).

A further increase of  $R$  ( $\approx 5$ – $6$ ) gives rise to a new signal in the  $^{199}\text{Hg}$  NMR spectra in the range 900–1100 ppm, indicating partial dissolution of **1** in excess of ammonia. The pH value of the solution increases significantly with  $R$  and reaches  $\text{pH} = 10$  already when  $R = 4$ . Obviously, mixed mercury(II) hydroxo and/or amido ( $\text{NH}_2^-$ ) species could then form.<sup>1</sup> The intensity of the signal grows continuously with increasing  $R$ , together with an increasing chemical shift of the  $^{199}\text{Hg}$  resonance, which approaches that of the  $[\text{Hg}(\text{NH}_3)_4]^{2+}$  complex in liquid ammonia at 298 K (cf. Table 3) (Figure 7). At  $R \approx 100$ , the mercury(II) concentration in the solution is  $0.09 \text{ mol} \cdot \text{dm}^{-3}$  and the chemical shift is 1205 ppm. Quantitative measurements of the mercury(II) concentration in solution could not be performed in the  $R$  range 3–5 where the chemical shift changes drastically. However, for  $R \leq 2$  with  $\delta(^{199}\text{Hg}) \approx 0$  ppm, the predominant mercury(II) species is  $[\text{Hg}(\text{H}_2\text{O})_6]^{2+}$ .

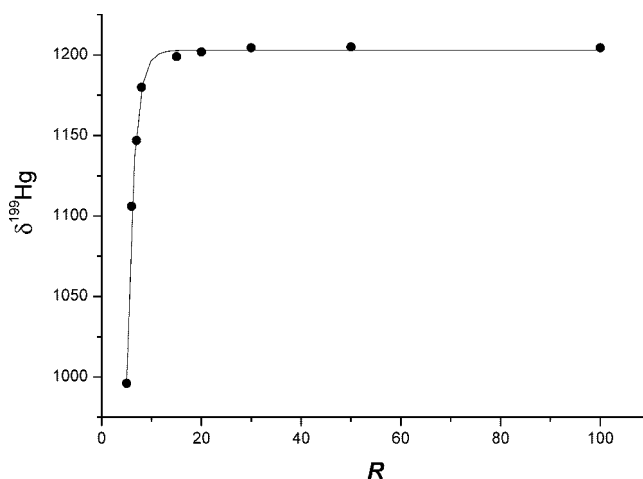


**Figure 7.** Dependence of the  $^{199}\text{Hg}$  chemical shift in the filtrate of the  $\text{Hg}(\text{ClO}_4)_2(\text{aq})\text{--NH}_3(\text{aq})$  system on the original net molar ratio  $R = n(\text{NH}_3)/n(\text{Hg}^{2+})$  in the heterogeneous system. The mercury(II) concentration in the solutions varied in the range 0.05–0.09 M.

The observed variation in the chemical shift of the  $^{199}\text{Hg}$  NMR signal is obviously caused by several species differing in the number of ammonia (amide) and water (hydroxo) ligands in the inner coordination sphere of the mercury(II) ion. The single  $^{199}\text{Hg}$  resonance shows that the solvent/ligand exchange is fast on the  $^{199}\text{Hg}$  NMR time scale. Solvates of the  $\text{d}^{10}$  mercury(II) ion are usually very labile in solution with very fast exchange rates of solvent molecules,<sup>40</sup> e.g., the mean residence time,  $\tau_e$ , of a water molecule in the hydrated mercury(II) ion is  $2 \times 10^{-9}$  s.<sup>19,41</sup>

Fast ligand exchange and the strong dependence of the  $^{199}\text{Hg}$  chemical shift in a range of 1100 ppm on ligand concentration was previously reported also for the  $[\text{HgCl}_n]^{(2-n)+}$  complexes in aqueous solution.<sup>42</sup> Despite the variation in coordination geometries,  $\text{HgCl}_2$  linear,  $\text{HgCl}_3^-$  planar trigonal, and  $\text{HgCl}_4^{2-}$  tetrahedral,<sup>43</sup> the dependence of the derived  $^{199}\text{Hg}$  chemical shifts for each species on the number of chloride ligands to the mercury(II) ion is well approximated by a straight line.<sup>42</sup>

When aqueous ammonia is added directly on  $\text{Hg}(\text{ClO}_4)_2 \cdot \sim 3\text{H}_2\text{O}$  crystals (see the Experimental Section), the dissolution of the crystals is accompanied by slow precipitation of tetraamminemercury(II) perchlorate powder. As expected, the only species detected in solution by  $^{199}\text{Hg}$  NMR at the resulting high  $R$  values is the  $[\text{Hg}(\text{NH}_3)_4]^{2+}$  complex ( $\delta = 1204$  ppm), and the mercury(II) concentration may reach  $0.11 \text{ mol} \cdot \text{dm}^{-3}$ .

**Mercury(II) Trifluoromethanesulfonate–Aqueous Ammonia System.** In a similar way as for the  $\text{Hg}(\text{ClO}_4)_2 \cdot \sim 3\text{H}_2\text{O}/\text{NH}_3(\text{aq})$  system described above, the reaction between anhydrous mercury(II) trifluoromethanesulfonate and aqueous ammonia results in complete dissolution of the solid followed by precipitation of gray tetraamminemercury(II) trifluoromethanesulfonate (see above). The only species detected in solution by  $^{199}\text{Hg}$  NMR is the solvated  $[\text{Hg}(\text{NH}_3)_4]^{2+}$  complex ( $\delta = 1204$

(40) Richens, D. T. *The Chemistry of Aqua Ions*; John Wiley & Sons Ltd.: Chichester, UK, 1997; Chapter 1.

(41) Eigen, M. *Pure Appl. Chem.* **1963**, *6*, 97.

(42) Klose, G.; Volke, F.; Peinel, G.; Knobloch, G. *Magn. Reson. Chem.* **1993**, *31*, 548–551.

(43) Sandström, M. *Acta Chem. Scand.* **1977**, *31*, 141–150.

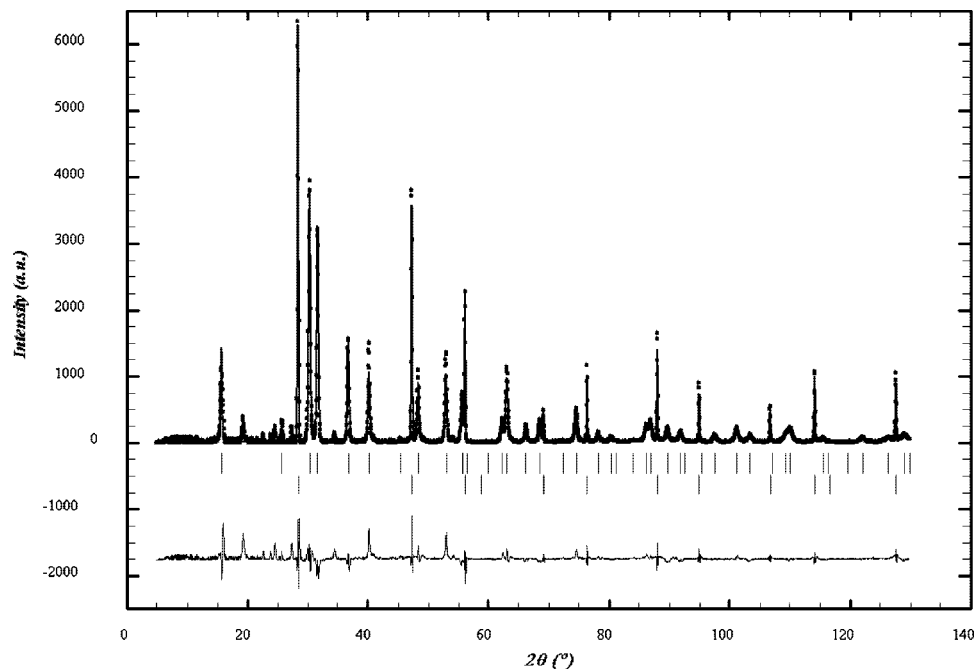


Figure 8. X-ray powder data and fit of Rietveld model refinements of **2**.

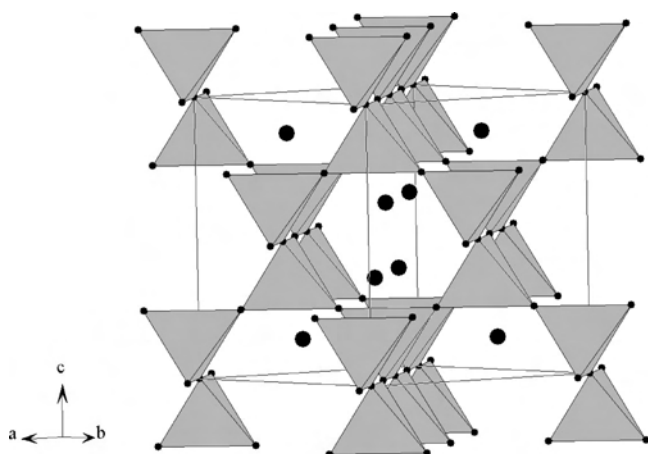


Figure 9. Network of Hg atoms in **2** with distances of 3.41 and 5.96 Å.

ppm). The solubility of the trifluoromethanesulfonate salt is approximately the same as for perchlorate; the mercury(II) concentration in concentrated ammonia solution of  $\text{Hg}(\text{CF}_3\text{SO}_3)_2$ ,  $R \approx 100$ , is  $0.12 \text{ mol} \cdot \text{dm}^{-3}$ .

**Structure of the Deammoniated Product 2.** The Rietveld analysis of the X-ray powder diffraction (XRD) data of **2** revealed only the positions of the mercury and the chlorine atoms. The perchlorate ions probably are subject to severe rotational disorder. An indication of this large dynamic disorder of the perchlorate ions is the huge thermal parameter for the chlorine atoms obtained in the Rietveld refinements. Furthermore, a few weak peaks in the beginning of the diffraction pattern indicate an ordered superstructure. Several plausible super cells with  $M$ -indexes above 10,<sup>44</sup> each with volumes in the order of 3 times the basic unit cell volume, could be found. However, we have not been able to uniquely determine the super structure cell.

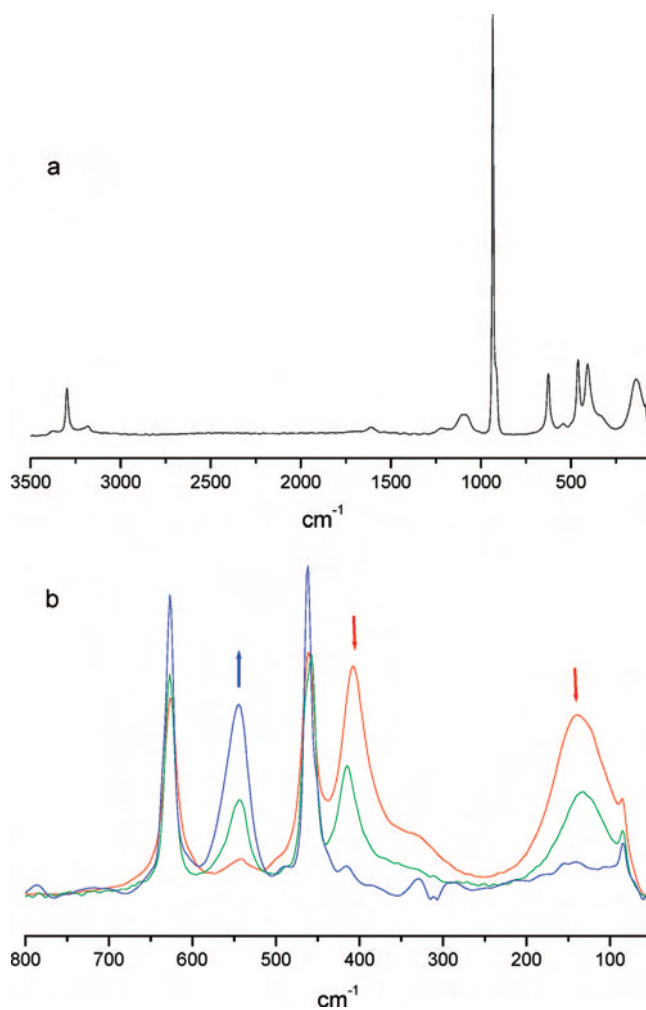


Figure 10. Raman spectra of **2**. (a) Full spectrum of finely ground crystals. (b) Low-frequency part of the spectrum, showing changes at heating: unheated (blue line), three times heated to 120 °C for 5 min (green line), three times heated to 120 °C for 10 min (red line).

(44) de Wolff, P. M. *J. Appl. Crystallogr.* **1968**, *1*, 108–113.

**Table 4.** IR and Raman Frequencies with Assignments of the  $[\text{Hg}(\text{NH}_3)_4](\text{ClO}_4)_2$  and  $[\text{Hg}(\text{NH}_3)_2](\text{ClO}_4)_2$  Compounds

group/bond	assignment	$[\text{Hg}(\text{NH}_3)_4](\text{ClO}_4)_2$					$[\text{Hg}(\text{NH}_3)_2](\text{ClO}_4)_2$	
		$\text{NH}_3(l)$	crystal <sup>a</sup>		powder <sup>b</sup>		Raman	IR
		Raman	Raman	IR	Raman	IR		
$\text{NH}_3$	$\nu_d$	3385 m	3380 w, br	3378 s	3370 w, sh	3375 m, br		3390 sh
	$\nu_s$	3295 s	3298 s	3293 s	3285 m	3289 m, sh	3211 m	3286 vs
	$2\delta_d$	3215 vs	3180 w, br	3205 m	3208 s	3178 w, br		
				3137 w				
	$\delta_d$	1641 m, br	1608 w	1617 m		1610 m		
	$\delta_s$	1055 m, br	1100 m, sh					
$\text{ClO}_4^-$	$\rho_r$			692 m, br				
				1424 w				1424 s
	$\nu_d$		1085 m, sh	1086 vs	1075 s	1077 s, br	1072 m, br	1087 vs
	$\nu_s$		934 vs	940 sh, b	938 vs	940 sh, br	938 vs	
	$\delta_d$		624 s	621 m	626 s	621 m	626 s	626 s
$\text{Hg}-\text{NH}_3$	$\delta_d$		461 s	461 vw	459 s		461 s	
	$\nu_s$		407 s	405 vw	407 s <sup>c</sup>		544 s	
			330 sh					455 vw
			135 s, br		132 s, br			

<sup>a</sup> Crystals from the  $\text{Hg}(\text{ClO}_4)_2 \cdot \sim 3\text{H}_2\text{O}-\text{NH}_3(l)$  system. <sup>b</sup> Powder from the  $\text{Hg}(\text{ClO}_4)_2(\text{aq})-\text{NH}_3(\text{aq})$  system. <sup>c</sup> When drying the powder samples at reduced pressure over silica gel for longer time, the  $408\text{ cm}^{-1}$  band is reduced while the  $544\text{ cm}^{-1}$  band grows; see text.

The formation of a linear N–Hg–N unit in **2** could immediately be established due to the characteristic prepeak of linear mercury(II) complexes present at 12 278 eV in the XANES spectrum (Figure S2 in the Supporting Information). It is also in agreement with the two short Hg–N bond distances of 2.064(8) Å obtained from the model curve-fitting of the EXAFS function (Table 2). Furthermore, the EXAFS model includes four equatorial Hg–O bond distances to oxygen atoms at a mean Hg–O bond distance of 2.84(2) Å. Most probably two perchlorate ions are bridging an infinite tetrahedral network of diamminemercury(II) entities (Figure 9). The shortest Hg···Hg distances were from EXAFS and XRD results found to be 3.420(4) and 3.45 Å, with longer distances between mercury atoms in two different “mercury-tetrahedra” at 5.96(1) and 5.96 Å, respectively. The chlorine atoms of the perchlorate ions were found at a distance of 4.06(3) (EXAFS) and 4.05 Å (XRD) from the mercury atoms, Figure 9.

A similar diamminemercury(II) entity is found in the structure of  $[\text{Hg}(\text{NH}_3)_2\text{Cl}_2]$ , which can be obtained by the action of aqueous ammonia on  $\text{HgCl}_2$ . The linear  $\text{NH}_3-\text{Hg}-\text{NH}_3$  entity has a Hg–N bond distance of 2.03 Å and four equatorial chloride ions with Hg–Cl of 2.87 Å to complete a distorted octahedral coordination.<sup>45</sup> The strongly covalent character of the Hg–N bond is indicated by the ease that a hydrogen ion can be removed from the ammine ligand to form amides, e.g. in  $\text{Hg}(\text{NH}_2)\text{Cl}$ , which contains infinite  $[\text{Hg}-\text{NH}_2^+]_\infty$  chains with bridging amido nitrogen atom between linear N–Hg–N entities.<sup>1</sup>

The monomeric complexes in the tetraamminemercury(II) and triamminesilver(I) perchlorate salts easily lose two and one ammonia molecules, respectively, to form quite stable diamminemercury(II) and diamminesilver(I) perchlorates.<sup>16,46</sup> These compounds consist of linear  $\text{M}(\text{NH}_3)_2$  entities connected in a network via weak perchlorate oxygen bridges; the structures are described above and in ref 18. These deammoniated

compounds are stable in wide temperature ranges and have low solubility in water, aqueous, and liquid ammonia.<sup>18</sup>

**Vibrational Spectra of the Mercury(II)–Ammine Complexes.** The vibrational frequencies obtained for the solid compounds from the mercury(II) perchlorate–liquid and aqueous ammonia systems are identical within the experimental uncertainty, confirming that the crystals and the precipitated powder contain the same compound,  $[\text{Hg}(\text{NH}_3)_4](\text{ClO}_4)_2$ . The frequencies are also compatible with the vibrational data recently reported for  $[\text{Hg}(\text{NH}_3)_4](\text{ClO}_4)_2$ .<sup>16</sup> The ammonia molecules give rise to intense bands in the N–H stretching region ( $3100\text{--}3500\text{ cm}^{-1}$ );<sup>47,48</sup> cf. Figure 10a and Table 4. The three characteristic high-frequency vibrations of ammonia are downshifted due to the coordination to the mercury(II) ion. The  $\text{ClO}_4^-$  frequencies are as expected for a noncoordinated perchlorate ions.<sup>48</sup> The strong band at  $\sim 407\text{ cm}^{-1}$  in the Raman spectra can be assigned to the Hg–N symmetric stretching mode, Figure 10b.

Deammoniation of the  $[\text{Hg}(\text{NH}_3)_2](\text{ClO}_4)_2$  compound has the strongest effect on the  $\nu(\text{N}-\text{H})$  and  $\nu(\text{Hg}-\text{N})$  frequencies (see Table 4). The Raman spectra show that when heating the  $[\text{Hg}(\text{NH}_3)_4](\text{ClO}_4)_2$  compound, the intensity of the  $\nu(\text{Hg}-\text{N})$  band at  $407\text{ cm}^{-1}$  is reduced, while a band at  $544\text{ cm}^{-1}$  that can be attributed to  $\nu(\text{Hg}-\text{N})$  of the  $\{[\text{Hg}(\text{NH}_3)_2(\text{ClO}_4)_2]_n\}$  compound grows (Figure 10b). This shift of the Hg–N symmetric stretching of  $\sim 137\text{ cm}^{-1}$  to higher frequency indicates that the Hg–N bonds are much stronger in the linear diammine complex.

## Conclusions

Mercury(II) perchlorate and trifluoromethanesulfonate form four-coordinated ammine complexes when dissolved in a large excess of ammonia, both in liquid and in concentrated aqueous ammonia solutions. The solvate crystallizing from such solutions contains the distorted

(45) MacGillavry, C. H.; Bijvoet, B. J. Z. *Kristallgr. Kristallgeom. Kristallphys. Kristallchem.* **1936**, *94*, 231.

(46) Nockemann, P.; Meyer, G. Z. *Anorg. Allg. Chem.* **2002**, *628*, 1636–1530.

(47) Gardiner, D. J.; Haji, A. H.; Straughan, B. J. *Chem. Soc., Dalton Trans.* **1978**, 705–710.

(48) Nakamoto, K. *Infrared and Raman Spectra of Inorganic and Coordination Compounds*, 5th ed.; Wiley-Interscience: New York, 1997.

tetrahedral  $[\text{Hg}(\text{NH}_3)_4]^{2+}$  complex, which easily loses two ammonia molecules to form a diammine with strongly coordinated linear  $[\text{H}_3\text{N}-\text{Hg}-\text{NH}_3]^{2+}$  entities when stored in air or heated.

**Acknowledgment.** We are grateful for the support from Dr. Mats Johnsson, Stockholm University, for carrying out the TG analyses and to Prof. Bo Liedberg, Department of Physics and Measurements, Linköping University, for the use of the Raman spectrometer. We gratefully acknowledge the financial support given to these investigations by the Swedish Research Council. Stanford Synchrotron Radiation Laboratory (SSRL) is gratefully acknowledged for allocation of beam-time and laboratory facilities at our disposal. SSRL is operated by the Department of Energy, Office of Basic Energy Sciences.

The SSRL Biotechnology Program is supported by the National Institutes of Health, National Center for Research Resources, Biomedical Technology Program, and by the Department of Energy, Office of Biological and Environmental Research.

**Supporting Information Available:** Distribution of complexes in the mercury(II)–ammonia system in water, normalized XANES spectra and Fourier transforms of the EXAFS data for samples studied by X-ray absorption spectroscopy, UV–vis spectra of liquid and aqueous ammonia mercury(II) perchlorate solutions, a table of hydrogen bonds in  $[\text{Hg}(\text{NH}_3)_4](\text{ClO}_4)_2$ , and the crystallographic information file text for the  $[\text{Hg}(\text{NH}_3)_4](\text{ClO}_4)_2$  structure at 293 K. This material is available free of charge via the Internet at <http://pubs.acs.org>.

IC7013489